

1. 14 August 1996 (final accepted version)
2. Non-collinear magnetism in distorted perovskite compounds
3. I.V.Solovyev^{a,*}, N.Hamada^b, K.Terakura^c
4. ^aJRCAT-ATP, 1-1-4 Higashi, Tsukuba, Ibaraki 305, Japan
^bScience University of Tokyo, 2641 Yamasaki, Noda, Chiba 278, Japan
^cJRCAT-NAIR, 1-1-4 Higashi, Tsukuba, Ibaraki 305, Japan

5. Abstract

Using results of the band structure calculations in the local-spin-density approximation we demonstrate how the crystal distortions affect the magnetic structure of orthorhombically distorted perovskites leading to a non-collinear spin arrangement. Our results suggest that the non-collinearity of the spin magnetic moments, being generally small in LaMO_3 series with $M=\text{Cr-Fe}$, is large in SrRuO_3 .

6. *keywords*: Heisenberg exchange, Dzyaloshinskii-Moriya exchange, perovskite transition metal oxides, band structure calculations

7. *Corresponding author.

I.V. Solovyev
JRCAT-ATP, c/o NAIR
1-1-4 Higashi
Tsukuba, Ibaraki 305
JAPAN
Fax:+81-298-54-2788
E-mail: igor@jrcat.or.jp

Perovskite transition-metal oxides are known to be the most striking example of materials where magnetic, transport and structural properties are strongly coupled. The reciprocal influence of the spin and lattice degrees of freedom can be due to the spin-orbit interaction (SOI) or the orbital ordering effects [1]. Both mechanisms can be responsible for the non-collinear magnetic arrangement through the antisymmetric Dzyaloshinskii-Moriya exchange interaction [2] or through strong dependence of the interatomic exchange on the orbital ordering [1] resulting in pronounced non-Heisenberg behavior [3]. We consider the first possibility for several orthorhombically distorted perovskites with D_{2h}^{16} structure where the non-collinear magnetism is allowed by symmetry [4]. However, the magnitude of the effect itself depends on the relative strength of several magnetic interactions.

We use the LMTO Green's function technique in the real space and perturbative approach both for small deviations of the spin magnetization near the scalar-relativistic equilibrium and SOI. Then, the total energy change can be expressed analytically as $\delta E = E_H + E_{DM} + E_{MAE}$. The first term $E_H \simeq -1/2 \sum_{ij} J_{ij} \mathbf{e}_i \cdot \mathbf{e}_j$ (\mathbf{e}_i is the direction of the spin magnetization at the site i) describes the isotropic Heisenberg exchange interaction and appears in the second order with respect to nonuniform rotations of spins [5]. The magnetocrystalline anisotropy energy (MAE) firstly appears in the second order with respect to the SOI. The antisymmetric coupling $E_{DM} \simeq \sum_{i>j} \mathbf{d}_{ij} [\mathbf{e}_i \times \mathbf{e}_j]$ corresponds to the mixed type perturbation with respect to spin rotations and SOI [6].

J_{ij} and \mathbf{d}_{ij} parameters for LaMO_3 series with $M=\text{Cr-Fe}$ and SrRuO_3 are shown in Tables 1 and 2. General tendencies of the nearest neighbor interactions J_{ij} can be understood by using simple tight-binding arguments given in [7]. (i) $J_{ij} < 0$ at the half of the band filling: t_{2g} -type exchange interaction in LaCrO_3 (formal atomic configuration of Cr is $t_{2g}^3 e_g^0$), both t_{2g} and e_g interactions in LaFeO_3 ($t_{2g}^3 e_g^2$). (ii) $J_{ij} > 0$ at the beginning and at the end of the band filling: e_g exchange interaction dominating in LaMnO_3 ($t_{2g}^3 e_g^1$) [6]. (iii) $J_{ij} \sim 0$ around 1/3 and 2/3 of the band filling: SrRuO_3 case ($t_{2g}^4 e_g^0$). On the other hand, \mathbf{d}_{ij} parameters being proportional to the SOI are generally larger in SrRuO_3 . The structural factor defined by rotations of the MO_6 octahedra relative to each other is of the same

order of magnitude for all compounds considered here. Thus, for LaMO_3 compounds the Heisenberg exchange interaction is clearly the strongest, whereas for SrRuO_3 it is considerably smaller and comparable with the antisymmetric exchange.

It is particularly interesting in LaMnO_3 that the interlayer exchange coupling $J_{1B} = \sum_{j \in B} J_{1j}$ with j running over Mn atoms in the plane B in Fig.1 crucially depends on the Jahn-Teller distortion (JTD) and varies between ferro- (FM) and antiferromagnetic (AFM) [6]. For the pure compound, the AFM interlayer coupling stabilized by JTD is large enough ($J_{1B} \simeq -1.4\text{mRy}$ [6]) to overcome the antisymmetric interactions and the magnetic spin structure is nearly collinear. Weak FM canting due to the \mathbf{d}_{12} interaction and estimated as $\sin^{-1} |\alpha_c / J_{1B}|$ is less than 2° (see [6] for details). However, JTD is suppressed rapidly with the hole doping, directly affecting the interlayer coupling constant J_{1B} . At certain concentration of the holes one expects $|J_{1B}| \sim |\alpha_c|$ and large non-collinearity. This tendency qualitatively explains the appearance of the spin-canted AFM phase accompanying the AFM-to-FM transition in the low-doped manganites [8].

In conclusion, the non-collinear spin structure, imposed by general symmetry rules, is suppressed in LaMO_3 oxides by the strong isotropic exchange interaction. The latter is reduced in SrRuO_3 suggesting essentially non-collinear magnetic arrangement.

The work is partly supported by New Energy and Industrial Technology Development Organization (NEDO).

References

- [1] K.I.Kugel and D.I.Khomskii, Sov. Phys. Usp. **25**, 231 (1982).
- [2] I.Dzyaloshinskii, J. Phys. Chem. Solids **4**, 241 (1958); T.Moriya, Phys. Rev. **120**, 91 (1960).
- [3] E.L.Nagaev, Sov. Phys. Usp. **25**, 31 (1982).
- [4] D.Treves, Phys. Rev. **125**, 1843 (1962).
- [5] A.I.Liechtenstein *et al.*, J. Magn. Magn. Mater. **67**, 65 (1987).
- [6] I.Solovyev *et al.*, Phys. Rev. Lett. **76**, 4825 (1996).
- [7] V.Heine and J.H.Samson, J. Phys. F: Metal Phys. **13**, 2155 (1983).
- [8] H.Kawano *et al.*, Phys. Rev. B **53**, 2202 (1996).

Table 1: Parameters of the isotropic exchange interaction J_{ij} (in mRy). Atomic positions 1, 2 and 3 are shown in Fig.1.

compound	J_{12}	J_{13}
LaCrO ₃	-1.321	-1.372
LaMnO ₃	0.225	0.668
LaFeO ₃	-2.559	-3.119
SrRuO ₃	0.306	-0.101

Table 2: Parameters of the antisymmetric exchange interaction \mathbf{d}_{ij} for two $M-O-M$ bonds (in mRy). The symmetry of the nearest neighbor interactions is shown in Fig.1.

compound	$\mathbf{d}_{12}:(-\alpha_{\mathbf{c}}, -\beta_{\mathbf{c}}, 0)$	$\mathbf{d}_{13}:(\alpha_{\mathbf{ab}}, -\beta_{\mathbf{ab}}, \gamma_{\mathbf{ab}})$
LaCrO ₃	(-0.005, -0.044, 0)	(0.029, -0.028, 0.035)
LaMnO ₃	(-0.032, -0.052, 0)	(0.032, -0.024, 0.039)
LaFeO ₃	(-0.019, -0.125, 0)	(0.075, -0.059, 0.086)
SrRuO ₃	(-0.138, -0.286, 0)	(-0.062, -0.127, 0.198)

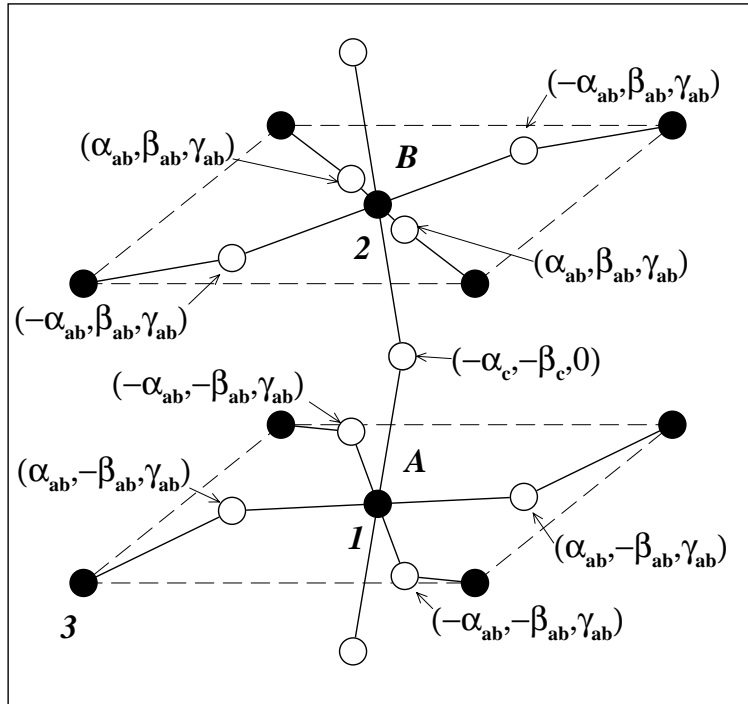


Figure 1: Parameters of the antisymmetric exchange interaction associated with different $M-O-M$ bonds in D_{2h}^{16} structure (black and white spheres are M and O respectively). α , β and γ are the components of \mathbf{d}_{ij} vectors along orthorhombic **a**, **b** and **c** axes for inplane (**ab**) and interplane (**c**) interactions.